Clauser Plot Method of Analysis on Molecular Tagging Velocimetry Data

Oriana R. Palumbo*
University of Tennessee Space Institute, Tullahoma, TN, 37388

The Clauser plot, or chart, method is a series of mathematical functions with the purpose of estimating the friction velocity, a necessary variable of the logarithmic-law of the wall. The log-law of the wall collapses fully turbulent boundary layers into wall coordinates, creating a dimensionless profile. This serves as a comparison to the canonical profile shown to be present in turbulent viscous flow. The main component required for this method is a velocity profile which may be obtained through several diagnostic methods, the details of which are outlined in this report. To gain a fundamental understanding of this method, it was applied to the undisturbed boundary layer state on the floor of University of Tennessee Space Institute's Mach 4 Ludwieg tube with data obtained through the use of molecular tagging velocimetry (MTV). The Clauser plot method provided information on boundary layer conditions for multiple similar data sets to determine consistency and accuracy. These preliminary results will set a foundation for future boundary layer characterization and serve as a reference condition for upcoming research that will explore the influence of surface heating on boundary layer growth and evolution.

I. Nomenclature

β	=	Clauser equilibrium parameter
C	=	Sutherland's constant
δ^+	=	dimensionless boundary layer height
κ	=	von Kármán constant
ρ_w	=	wall density
T_{aw}	=	adiabatic wall temperature
T_w	=	wall temperature
T_0	=	reference temperature
T_∞	=	free stream static temperature
τ	=	shear stress
U_{eff}	=	van Driest effective velocity
U_τ	=	friction velocity
U_∞	=	free stream velocity
U^+	=	boundary layer velocity in wall coordinates
v_w	=	wall kinematic viscosity
Y	=	measured wall normal location
Y^+	=	wall normal location in wall coordinates
y	=	theoretical wall normal location
μ	=	viscosity
μ_0	=	reference viscosity

II. Introduction

The state and behavior of the viscous boundary layer has profound effects on the aerodynamic performance of high-speed flight vehicles including impacts on drag, surface heating, and separation. As predictive computational tools improve and greater efficiency is sought in high-speed system design, improved understanding of the impact of realistic surface conditions on the boundary layer is required. Experimental diagnostics used in high-speed wind tunnels

*Graduate Research Assistant, Department of Mechanical, Aerospace, and Biomedical Engineering, AIAA Student Member

Table 1 Run conditions in UTSI's Mach 4 Ludwieg tube

Diaphragms	Static Pressure (kPa)	Total Pressure (kPa)	Total Temperature (K)	Free Stream Velocity (m/s)	Re/L (1/m)
2	2.092	317.7	287.3	663	17.0×10^6
2	2.113	320.8	287.3	663	17.0×10^6

have the ability to validate and improve these advanced computational results. However, experimental techniques are limited by size constraints, atmospheric conditions, and durations on the scale of milliseconds. A critical challenge for investigating boundary layer development on wind tunnel models is the relatively small height of the boundary layer, making profile measurements extremely difficult and often poorly resolved. To mitigate this problem, more experimental analyses are being conducted on the thicker boundary layer along the tunnel floor.

Previously, Gragston and Smith performed acetone MTV on the floor of UTSI's Mach 4 Ludwieg tube and analyzed the data through the Clauser chart method [1]. Their experiment serves as a direct comparison to the presented results. However, there are more options for the application of the Clauser chart method. Velocity data may be similarly obtained from other diagnostics including krypton tagging velocimetry (KTV), femtosecond laser electronic excitation tagging (FLEET), and particle image velocimetry (PIV). All of these diagnostics involve tagging particles in a fluid and recording their propagation downstream. Depending on factors including cost budget and time, different facilities utilize different diagnostics. In a separate UTSI wind tunnel facility, PIV is readily available and requires little setup time, so it is often used there [2]. In this case, MTV is readily available for the Mach 4 Ludwieg tube, so it could be prepared under a relatively short time frame, leaving more time for data collection. Krypton MTV can be a similar and improved alternative to acetone MTV as it has a longer illumination lifespan and is less likely to chemically react in hypersonic facilities [3]. However, this method can be more expensive [1]. In addition to these, FLEET is also a reliable option for obtaining velocity profiles. This diagnostic does not require seeding, instead illuminating the nitrogen present in atmospheric air. Eliminating this step provides an advantage as uneven mixing of seeded particles is no longer a concern. Another key difference between FLEET and MTV is that MTV operates through the use of a Nd:YAG laser while FLEET requires a femtosecond laser, so experimental capabilities rely on the availability of each of these lasers [4].

Despite the Clauser chart method's versatility in diagnostic applications, it does possess some limitations and assumptions that should be noted. Wei et al. provide evidence that as Reynolds number increases, the difference between true calculated friction velocity and the friction velocity provided by the Clauser chart method increases [5]. The provided explanation for such a phenomenon suggests that the Clauser chart method operates under the assumption that the universal logarithmic-law of the wall holds true, which is not always the case and especially with higher Reynolds numbers. This method also fails to resolve accurate velocity profiles in flows with varying pressure conditions normal to the wall, and thus is not advised to be implemented in situations involving strong pressure gradients [6]. However, each of these flaws can be mitigated through the formation of a non-universal log-law modified specifically for these situations.

III. Experimental Setup

A. Wind Tunnel Facility

The Mach 4 Ludwieg Tube facility in the Tennessee Aerothermodynamics Laboratory (TALon) at UTSI was used to obtain molecular tagging velocimetry data. This high-speed wind tunnel has a relatively large size with a 24 x 24 x 72 inch test section containing a fully turbulent boundary layer roughly 3 inches thick. It can produce steady state conditions for 105-125 ms per run and operates through the use of a vacuum system and compressed driver tube separated by a 23.25 inch Mylar diaphragm. While the vacuum system reduces the downstream test section of the tunnel to a pressure near 0 psi, the upstream driver tube pressure is raised, with a safety limit at 75 psi [7]. Once there is a substantial enough change in pressure between these two portions, the diaphragm ruptures, marking the start of the short run duration. This diaphragm can be 1-3 layers thick, with more layers correlating with increasing Reynolds numbers. Two MTV wind tunnel experiments completed in this facility are indicated in Table 1.

B. Molecular Tagging Velocimetry

MTV can be done through the use of many different seeded particles including acetone, water vapor, nitrogen dioxide, ozone, and biacetyl [8]. For the purpose of this experiment, acetone was chosen to be seeded through the use of a bubbler (Fig. 1). The bubbler is filled with 100 milliliters of liquid acetone which is then aerated and dispersed into the wind tunnel upstream of the test section. As it travels downstream, this acetone is illuminated in a process called laser induced phosphorescence [8]. Aiming the laser at the acetone gas causes these molecules to become excited, shifting their electrons up a level before they eventually return to a ground state. Phosphorescence involves a triplet exited state that contains less light intensity yet lasts longer than florescence [9]. Florescence occurs when seeding the flow with chemicals dissociated from molecules, while phosphorescence involves complete molecules, such as acetone.

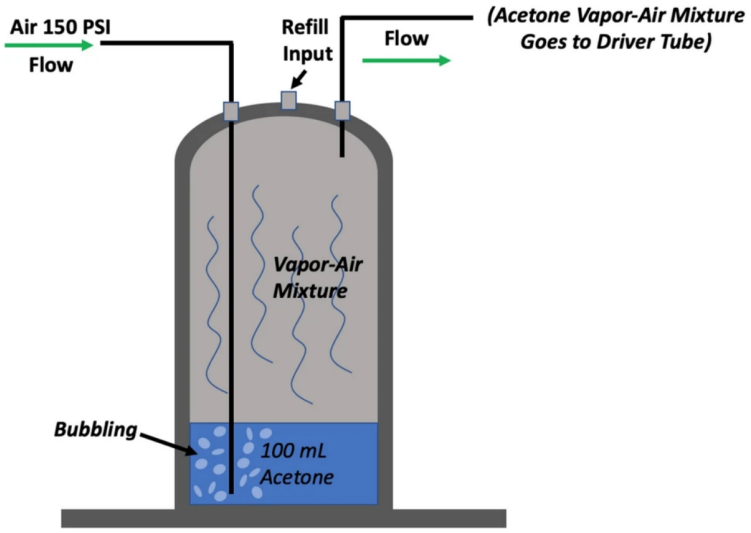

Fig. 1 Acetone seeding bubbler [1].

To properly tag a line of molecules, the proper excitation wavelength must be introduced to the seed particle. In the case of acetone, this wavelength is around 266 nanometers which is achieved by a Nd:YAG pulse burst laser bursting at a fixed interval [1]. In order for this process to work, the burst interval of the laser must be slower than the imaging system's frame rate. Then, each frame will contain several visible lines of acetone when imaged with an intensifier attachment included on the high-speed camera. Without the intensifier, the recorded frames would only include one line each. These lines and how far they move are what provide the velocity data (Fig. 2). If the laser burst rate is known as well as the physical distance between illuminated lines of acetone, then distance over time data can be extrapolated. These distance measurements are made possible through the use of a calibration ruler. By taking a photo of the ruler and measuring a pixel to physical length conversion, then the experimental data can be measured in that physical quantity.

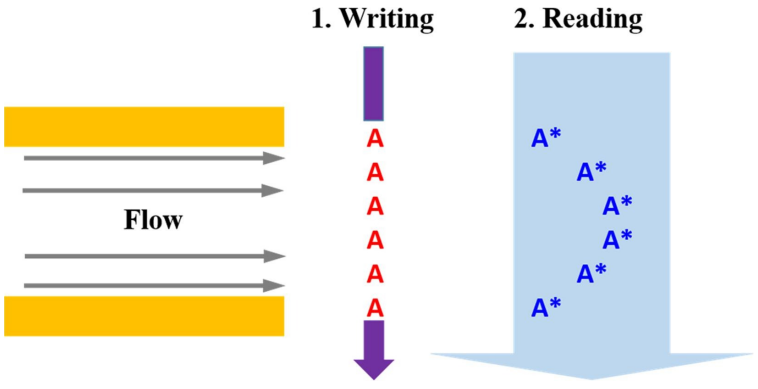

Fig. 2 The laser induced "write line" projects downstream into a velocity profile [8], [10].

In order to gain velocity data from the obtained images, all frames must be processed through a code that finds each line of pixels that is illuminated, calculates the distance between each of them, and uses an inputted laser burst interval and length calibration. When there are hundreds to thousands of frames to process, this calculation is expedited through average imaging. For this, a steady state range must be defined for averaging frames over. If all frames are averaged, then discontinuities may arise which interfere with the data and cause inaccuracies. Collecting velocity data from one average image makes the entire process much simpler, though it eliminates unsteady information if it exists.

C. Clauser Plot Method

The Clauser plot method code begins with the velocity profile obtained from the MTV data, importing the velocity and wall normal heights. Also included in the information provided to the code are standard conditions including the specific heat ratio, universal gas constant, wall temperature, atmospheric conditions inside the tunnel, and more. The first notable programmed equation is Sutherland's equation, revealing the density at the wall and by extension the wall kinematic viscosity (Eq. 1). Here, μ_0 represents the reference viscosity 1.716x10^{-5} N*s/m^2, C is Sutherland's constant at 110.4 K, and T_0 is a reference temperature 273 K. Before the Clauser chart method begins, velocity must be transformed into effective velocity developed by van Driest [11]. This step is crucial as it validates the logarithmic-law of the wall for compressible flows where density varies with respect to height [12]. This formula requires several temperature values: free stream temperature, wall temperature, and adiabatic wall temperature (Eq. 2). The adiabatic wall temperature is calculated using equation 4 and is based on the recovery factor method using the cube root of the Prandtl number [1]. After the velocity data is transformed into the appropriate effective velocity, the logarithmic-law of the wall can be applied to non-dimensionalize the velocity and height components of the boundary layer velocity profile into wall coordinates, a process dependent on the friction velocity. Performing this conversion reveals the three different segments of the boundary layer: the inner, overlap, and outer layer shown below in wall coordinates (Fig. 3). When the log-law of the wall is applied to the velocity profile, these three segments become visible with the requirement of logarithmic velocity on the x axis [12].

$$\mu = \frac{\mu_0 \left(\frac{T_w}{T_0}\right)^{3/2} (T_0 + C)}{C + T_w} \tag{1}$$

$$U_{eff} = \frac{U_\infty}{B_1}\left[sin^{-1}\left(\frac{2B_1^2\frac{U_\tau}{U_\infty} - B_2}{B_3}\right) + sin^{-1}\left(\frac{B_2}{B_3}\right)\right] \tag{2}$$

$$B_1 = \frac{T_{aw} - T_\infty}{T_w} \qquad B_2 = \frac{T_{aw}}{T_w} - 1 \qquad B_3 = \sqrt{B_2^2 + 4B_1^2} \tag{3}$$

$$T_{aw} = Pr^{1/3}(T_0 - T_\infty) + T_\infty \tag{4}$$

The inner portion of the velocity profile at the wall is dominated by viscous forces whose velocity appears to grow exponentially as distance from the wall increases, confirming the no slip condition. The overlap layer includes both viscous and turbulent eddies that create a linear relation on the semi-logarithmic plot. The outer layer, dominated by turbulent eddies, asymptotically approaches a limit at the free stream velocity. The log-law formula requires two additional constants to function, kappa and beta. Kappa is typically known to be 0.41 and beta is usually kept at 5.0 for a smooth surface [1, 12]. These values are included in the log-law formula below in equation 6. This equation is the highlight of the Clauser chart method, a style of least squares regression with the purpose of estimating the shear stress and friction velocity at the wall. This friction velocity, calculated by equation 5, is the value used to non-dimensionalize the velocity profile into the logarithmic-law of the wall.

$$U_\tau = \sqrt{\frac{\tau}{\rho_w}} \tag{5}$$

$$U^+ = \frac{1}{\kappa} log(Y^+) + \beta \qquad Y^+ = \frac{y * U_\tau}{\nu_w} \tag{6}$$

$$U^+ = \frac{U_{eff}}{U_\tau} \qquad Y^+ = \frac{Y * U_\tau}{\nu_w} \tag{7}$$

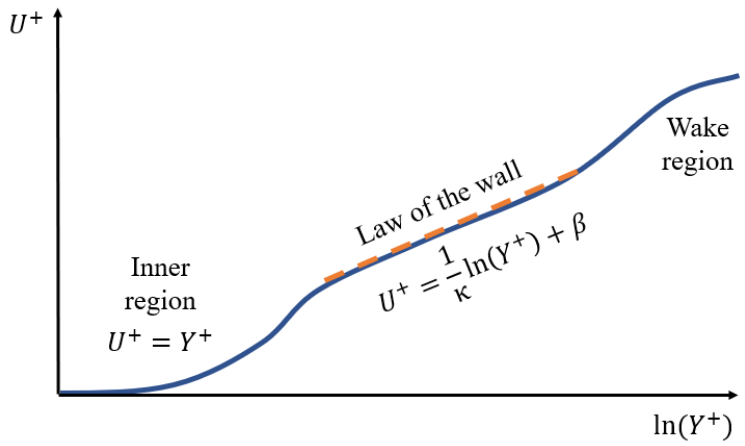

Fig. 3 Logarithmic-law of the wall with the inner, overlap, and outer regions.

This least squares method iterates through various shear stress values in a given range to determine what value of shear stress moves the profile closest to the expected theoretical law of the wall values. These theoretical values are calculated from two equations involving a notional, realistic range of boundary layer heights and the two previously mentioned constants kappa and beta (Eq. 6). When plotted onto a semi-logarithmic chart, these two formulas provide values for the velocity and height axes that form a linear relation. Using two slightly different law of the wall equations for the measured experimental values condenses the provided velocity profile into a similar linear relation (Eq. 7). Each of these equations contains guessed values of shear stress, a component of friction velocity. When these data driven profiles are iterated through the least squares regression the distances between these two profiles are documented and the shear stress providing the least difference in position is chosen as the accepted value. Both law of the wall equations, theoretical and experimental, are then calculated again and plotted using this value [13].

IV. Results and Discussion

The Clauser chart program was applied to the before mentioned tunnel campaigns with similar degrees of success. The velocity profiles gained from each of these experiments are provided below in Figure 4. The wide uncertainty ranges are due to the scaling factor in the pixel to length conversion ratio found by imaging a precise ruler and measuring the amount of pixels between two points on the ruler. One indicator on this ruler may be several pixels wide, leading to potential errors when calculating the distance traveled by each line of acetone. The dimensionless profiles appear to be valid as the slope of the MTV data matches the slope of the theoretical log-law of the wall (Fig. 5). The second case contains more sporadic velocities, but these originate from deep within the boundary layer where MTV becomes more unreliable. The lower cutoff of the slope also in this case could indicate an error in boundary layer height as the data may be shifted down as suggested when comparing the velocity profiles from both tests.

Some uncertainties arise from the choice of values for constants in the log-law of the wall (Eq. 6). Segalini et al. utilize a von Kármán constant of $\kappa = 0.38$ and an additive constant of $\beta = 4.1$ and determine uncertainty bounds based on these values for much lower Reynolds numbers [14]. Because prior usage of the Clauser chart method in the Mach 4 Ludwieg tube has been documented with valid results, the constants $\kappa = 0.41$ and $\beta = 4.1$ were specified for this analysis due to the previous work of Gragston and Smith [1]. Although the data lines up with expected values, hidden errors may still arise if the original data requires an adjusted form of the log-law. Preceding these possible errors, another uncertainty originates from initial data collection. Because MTV relies on adequate and homogeneous mixing of acetone, boundary layers with substantially vortical flows have the capability of providing inaccurate velocity profiles. If the profile line revealed the average velocity of all particles in the boundary layer, this issue would be minimized. Unfortunately, MTV data provides information on one line of particles, although this can be helpful in some cases. Overall, these results were insightful and provided an initial assessment of this method's application to MTV data and how to improve it.

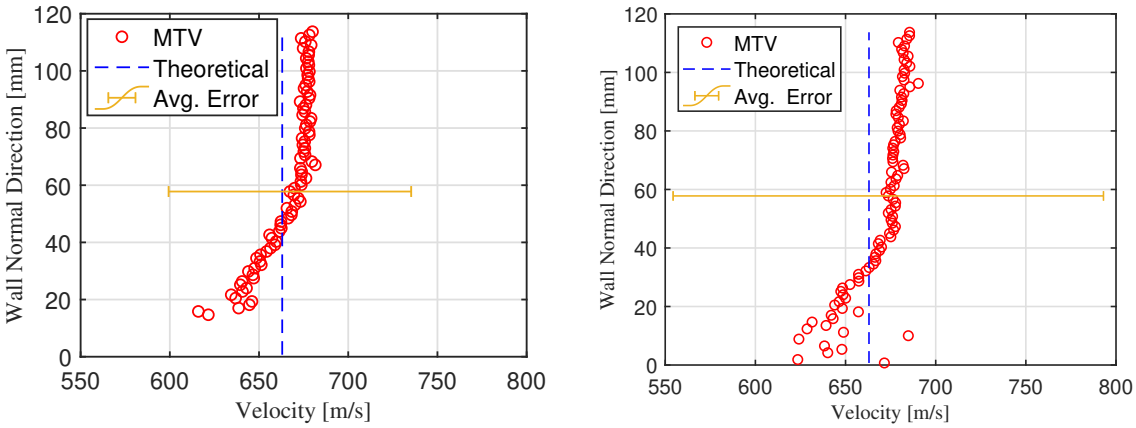

(a) Run 1 (b) Run 2

Fig. 4 Molecular tagging velocimetry data generated velocity profiles.

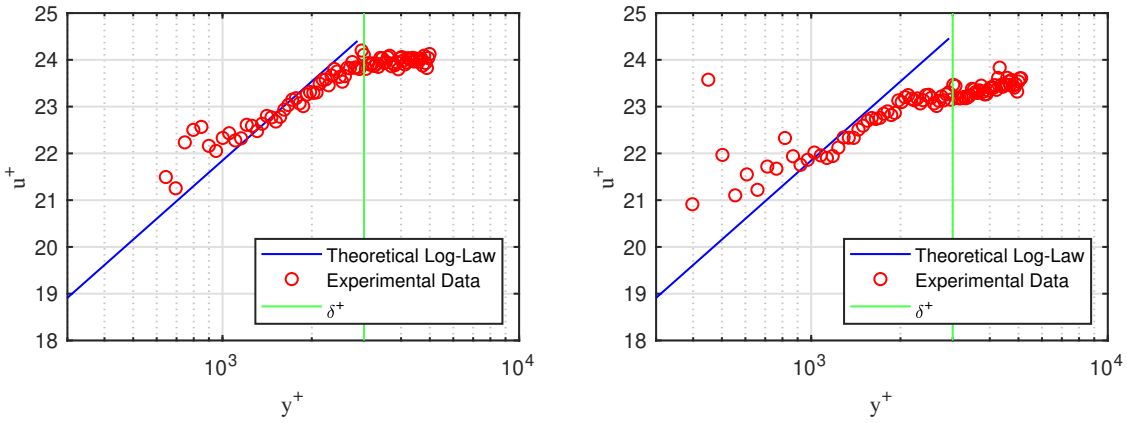

(a) Run 1 (b) Run 2

Fig. 5 Semi-logarithmic dimensionless velocity profiles.

V. Conclusion

The purpose of this study was to establish a baseline understanding of the Clauser chart method approach to boundary layer characterization and share this knowledge with UTSI's student body. Because the state of the boundary layer has a significant effect on flight vehicle performance, possessing a program that reveals information on the validity of recorded data within a short time frame is essential. When completing a wind tunnel experiment, it is crucial to investigate the data as it is being collected so any necessary adjustments can be made to the system. This code will help mitigate the amount of tunnel re-entries after data is deemed unusable post-clean up. Along with providing a quick visualization of data results, it can also be used to compare characterized boundary layers with previously published boundary layer results due to its non-dimensional structure. These comparisons can be made not only with experimental data, but with data originating from computational fluid dynamics as well, allowing for a direct link between experimental and computational results.

Now that the best value of shear stress for the undisturbed boundary layer has been determined, this method can be used to observe boundary layer profile changes resulting from various surface conditions including surface heating and roughness. To further investigate this, the Clauser chart program will be used in multiple future boundary layer profile analyses with increasing complexity. Observing how the Clauser chart method retains its validity and modifying it to represent several flow fields, including varying Reynolds numbers, is also included in the future of this campaign.

This will be accomplished by exposing the program to several wind tunnel facilities, various boundary layer sizes and structures, and more diagnostic methods. The code will be provided to UTSI where it may be used and improved upon by several projects, supporting future advanced boundary layer research.

Acknowledgments

The author would like to thank Meg Buckner and Kyle Klingaman for providing the MTV data for this analysis and Dr. Mark Gragston for his assistance in developing this program. The author would also like to thank Dr. John Schmisseur for his support and guidance in this project.

References

[1] Gragston, M., and Cary, S., "10 kHz molecular tagging velocimetry in a Mach 4 air flow with acetone vapor seeding," *Experiments in Fluids*, Vol. 63, No. 85, 2022. https://doi.org/10.1007/s00348-022-03438-1.

[2] Williams, O. J. H., Nguyen, T., Schreyer, A.-M., and Smits, A. J., "Particle response analysis for particle image velocimetry in supersonic flows," *Physics of Fluids*, Vol. 27, No. 7, 2015, p. 076101. https://doi.org/10.1063/1.4922865.

[3] Parziale, N. J., Smith, M. S., and Marineau, E. C., "Krypton tagging velocimetry of an underexpanded jet," *Applied Optics*, Vol. 54, No. 16, 2015, pp. 5094–5101. https://doi.org/10.1364/AO.54.005094.

[4] Danehy, P. M., Burns, R. A., Reese, D. T., Retter, J. E., and Kearney, S. P., "FLEET Velocimetry for Aerodynamics," *Annual Review of Fluid Mechanics*, Vol. 54, No. 1, 2022, pp. 525–553. https://doi.org/10.1146/annurev-fluid-032321-025544.

[5] Wei, T., Schmidt, R., and Mcmurtry, P., "Comment on the Clauser chart method for determining the friction velocity," *Experiments in Fluids*, Vol. 38, 2005, pp. 695–699. https://doi.org/10.1007/s00348-005-0934-3.

[6] Dixit, S., and Ramesh, O., "Determination of skin friction in strong pressure-gradient equilibrium and near-equilibrium turbulent boundary layers," *Experiments in Fluids*, Vol. 47, 2009. https://doi.org/10.1007/s00348-009-0698-2.

[7] Kreth, P. A., Gragston, M., Davenport, K., and Schmisseur, J. D., "Design and Initial Characterization of the UTSI Mach 4 Ludwieg Tube," *AIAA Scitech 2021 Forum*, 2021. https://doi.org/10.2514/6.2021-0384.

[8] Li, F., Zhang, H., and Bai, B., "A review of molecular tagging measurement technique," *Measurement*, Vol. 171, 2021. https://doi.org/10.1016/j.measurement.2020.108790.

[9] Lakowicz, J., "Instrumentation for Fluorescence Spectroscopy," *Principles of Fluorescence Spectroscopy*, 2006, pp. 27–61.

[10] Pitz, R., Wehrmeyer, J., Ribarov, L., and Oguss, D., "Unseeded molecular flow tagging in cold and hot flows using ozone and hydroxyl tagging velocimetry," *Measurement Science and Technology*, Vol. 11, No. 9, 2000. https://doi.org/10.1088/0957-0233/11/9/303.

[11] van Driest, E., "On Turbulent Flow Near a Wall," *Journal of the Aeronautical Sciences*, Vol. 23, No. 11, 1956, pp. 1007–1011. https://doi.org/10.2514/8.3713.

[12] White, F. M., and Majdalani, J., *Viscous Fluid Flow*, Vol. 3, McGraw-Hill New York, 2006.

[13] Clauser, F. H., Dryden, H., and von Kármán, T., "The Turbulent Boundary Layer," Elsevier, 1956, pp. 1–51. https://doi.org/https://doi.org/10.1016/S0065-2156(08)70370-3.

[14] Segalini, A., Örlü, R., and Alfredsson, P.-H., "Uncertainty analysis of the von Kármán constant," *Experiments in Fluids*, Vol. 54, 2013, p. 1460. https://doi.org/10.1007/s00348-013-1460-3.